

# Laser-Induced Choroidal Neovascularization in Mice Attenuated by Deficiency in the Apelin-APJ System

Chikako Hara,<sup>1</sup> Atsushi Kasai,<sup>2</sup> Fumi Gomi,<sup>1</sup> Tatsuya Satooka,<sup>2</sup> Susumu Sakimoto,<sup>1</sup> Kei Nakai,<sup>1</sup> Yasuhiro Yoshioka,<sup>2</sup> Akiko Yamamuro,<sup>2</sup> Sadaaki Maeda,<sup>2</sup> and Kohji Nishida<sup>1</sup>

<sup>1</sup>Department of Ophthalmology, Graduate School of Medicine, Osaka University, Suita, Osaka, Japan

<sup>2</sup>Department of Pharmacotherapeutics, Faculty of Pharmaceutical Sciences, Setsunan University, Hirakata, Osaka, Japan

Correspondence: Fumi Gomi, Department of Ophthalmology, Graduate School of Medicine, Osaka University, 2-2 Yamadaoka, Suita, Osaka 565-0871, Japan; fgomi@ophthal.med.osaka-u.ac.jp.

CH and AK contributed equally to the work presented here and should therefore be regarded as equivalent authors.

Submitted: January 6, 2013

Accepted: May 23, 2013

Citation: Hara C, Kasai A, Gomi F et al. Laser-induced choroidal neovascularization in mice attenuated by deficiency in the apelin-APJ system. *Invest Ophthalmol Vis Sci.* 2013;54:4321-4329. DOI:10.1167/iovs.13-11611.

**PURPOSE.** To investigate the role of the apelin-APJ system in the development of choroidal neovascularization (CNV).

**METHODS.** Experimental CNV was induced by laser photocoagulation in wild-type (WT), apelin-deficient (apelin-KO), and apelin receptor (APJ)-deficient (APJ-KO) mice. The gene expression levels of angiogenic or inflammatory factors were determined by quantitative real-time reverse transcription-polymerase chain reaction. APJ expression in CNV lesions was examined by immunohistochemistry. The sizes of the CNV lesions in the three mouse models were measured and compared histologically using isolectin B4 staining. Macrophage recruitment was measured by flow cytometric analysis. Proliferation of endothelial cells was determined using the alamar Blue assay.

**RESULTS.** Laser photocoagulation significantly increased expression of apelin and APJ in the retina-retinal pigment epithelium (RPE) complex. APJ immunoreactive cells were found in the CNV lesions and colocalized with platelet endothelial cell adhesion molecule-1, an endothelial cell marker. The sizes of the CNV lesions in apelin-KO or APJ-KO mice decreased significantly compared with those in the WT mice. Macrophages in the RPE complex of the apelin-KO mice, in which gene expression of the inflammatory factors was almost equal to that in WT mice, were recruited as a result of laser photocoagulation to the same degree as in WT mice. In addition, apelin small and interfering RNA (siRNA) suppressed proliferation of endothelial cells independently of vascular endothelial growth factor (VEGF) receptor 2 signaling, while VEGF increased expression of apelin and APJ in human umbilical vein endothelial cells.

**CONCLUSIONS.** The results suggested that the apelin-APJ system contributes to CNV development partially independent of the VEGF pathway.

**Keywords:** apelin, APJ, choroidal neovascularization, vascular endothelial growth factor, age-related macular degeneration

Exudative age-related macular degeneration (AMD), a major cause of severe visual loss in developed countries,<sup>1,2</sup> is characterized by choroidal neovascularization (CNV), in which new blood vessels grow from the choroid through Bruch's membrane into the subretinal space. CNV develops as a result of a combination of inflammatory and angiogenic processes.<sup>3,4</sup> Although many factors in the inflammatory and angiogenic cascade have been identified as regulators of CNV development, vascular endothelial growth factor (VEGF), a potent angiogenic factor, is currently the most effective therapeutic target for exudative AMD in clinical practice.<sup>5-8</sup>

Apelin was first identified as an endogenous ligand of the orphan G-protein-coupled receptor APJ,<sup>9</sup> and was highly expressed in the endothelial cells at the tips of growing capillaries, where APJ mediates the paracrine effects of apelin in the endothelial cells.<sup>10-12</sup> We showed for the first time that apelin stimulates the proliferation and migration of retinal endothelial cells, and this promotes vascular tube formation.<sup>13</sup> Recently, the possible role of the apelin-APJ system in physiologic or pathologic angiogenesis (development,<sup>11,14-17</sup> tumor development,<sup>14,18,19</sup> hypoxia<sup>13,20,21</sup>) has received much attention. We

previously reported that the apelin-APJ system facilitates intraocular angiogenesis, especially endothelial cell proliferation.<sup>16,20</sup> Moreover, it has been reported that the apelin-APJ system has crosstalk with VEGF signaling.<sup>14,20,22</sup> In addition to experimental studies, recent clinical studies have suggested that the apelin-APJ system is involved in retinal angiogenesis in proliferative diabetic retinopathy.<sup>23</sup> However, the role of the apelin-APJ system in CNV development has not been determined.

In the current study we investigated the involvement of the endogenous apelin-APJ system in CNV development in a well-established murine model of laser-induced CNV. Moreover we confirmed crosstalk between the VEGF pathway and apelin-APJ system using endothelial cells and endothelial cell proliferation assay.

## METHODS

### Animals

All animal experiments followed the guidelines of the ARVO Statement for the Use of Animals in Ophthalmic and Vision

**TABLE.** Predeveloped TaqMan Assay Reagent (Quantitative PCR)

Glyceraldehyde 3-phosphate dehydrogenase (GAPDH) for mouse	Mm99999915
Apelin for mouse	Mm00443562
APJ for mouse	Mm00442191
Vascular endothelial growth factor-A (VEGF-A) for mouse	Mm01281449
Vascular endothelial growth factor receptor 2 (VEGFR2) for mouse	Mm01222421
Monocyte chemoattractant protein-1 (MCP-1) for mouse	Mm00441242
Tumor necrosis factor- $\alpha$ (TNF- $\alpha$ ) for mouse	Mm00443258
GAPDH for human	Hs99999905
Apelin for human	Hs00175572
APJ for human	Hs00270873
VEGF-A for human	Hs00900055

Research and were approved by the Committee for the Ethical Use of Experimental Animals at Setsunan University and Osaka University. C57BL/6 mice were purchased from Japan SLC, Inc. (Hamamatsu, Japan). Apelin-deficient (apelin-KO) and APJ-deficient (APJ-KO) mice were generated by gene targeting.<sup>20</sup> Adult male mice (8–10 weeks old) were used in all experiments. The mice were housed in metal breeding cages in a room with a 12-h/12-h light/dark cycle. The humidity and temperature were maintained at 55% and 23°C, respectively; the mice had free access to food and water. Genotypes were confirmed by polymerase chain reaction (PCR) of genomic DNA extracted from tail snips. Every effort was made to minimize animal discomfort, reduce the number of animals used, and use alternatives to in vivo techniques.

### Laser-Induced CNV

Laser-induced CNV was generated by a previously described technique with some modifications.<sup>24</sup> The mice were anesthetized by intraperitoneal administration of a mixture of medetomidine (0.3 mg/kg), midazolam (4 mg/kg), and butorphanol (5 mg/kg). A mixture of 0.5% tropicamide and 0.5% phenylephrine hydrochloride (Mydrin P; Santen Pharmaceutical Co. Ltd., Osaka, Japan) was instilled in both eyes to dilate the pupils. Laser coagulation was performed for wild-type (WT) and apelin-KO mice (659 nm, 150 mW, 0.1-second duration, 50  $\mu$ m spot size [MC-300; Nidek, Gamagori, Japan]) (lesion size studies, four spots/eye; flow cytometry, 25 spots/eye; gene expression studies, 10 spots/eye) and for APJ-KO mice (514 nm, 100 mW, 0.05-second duration, 50  $\mu$ m spot size [Ultima 2000 SE, Lumenis, Santa Clara, CA]) (lesion size studies, six spots/eye) in both eyes of each animal to induce CNV as described previously.<sup>25,26</sup> Laser spots were applied in a peripapillary distribution in a standardized fashion approximately one to two disc diameters from the optic nerve using a slit-lamp delivery system (SL130; Carl Zeiss, Tokyo, Japan). The appearance of a cavitation bubble, which is correlated with disruption of Bruch's membrane, was recorded. Spots with hemorrhagic complications were excluded from further evaluation.

### Quantitative PCR to Measure Transcription Levels

At 2, 4, and 7 days after laser photocoagulation, the eyes were enucleated, and the anterior segment, muscles, and optic nerves were removed to isolate the eye cups (retina-retinal pigment epithelium [RPE] complex). Total RNA was extracted from the eye cups using an RNeasy Plus Mini Kit (Qiagen, Valencia, CA); reverse transcription (RT) of 1.0  $\mu$ g total RNA was performed with Super Script III Reverse Transcriptase (Invitrogen, Karlsruhe, Germany). All gene transcripts were quantified using quantitative real-time RT-PCR with ABI 7500 (Applied Biosystems, Foster City, CA). Real-time RT-PCR was

done using TaqMan assays (Applied Biosystems). The quantitative expression of each cytokine was calculated by a standard curve for target genes and glyceraldehyde 3-phosphate dehydrogenase (GAPDH). The primers and probes for mice are listed in the Table.

### Histology and Immunohistochemistry

Eyes obtained from mice euthanized 7 days after laser photocoagulation were fixed in zinc fixative (BD Pharmingen, San Diego, CA), paraffin embedded, and sectioned (58- $\mu$ m thickness) for histologic and immunohistochemical processing. After the anterior segment and neural retina were removed, four to six radial cuts were made from the edge to the equator, and the eye cup was flat mounted with the sclera facing down. For histologic analysis, the sections and the choroidal flat mounts were stained with hematoxylin and eosin. For double labeling, paraffin-embedded eyes were sectioned, followed by blocking with Tris-buffered saline containing 0.5% Triton X-100 and mouse IgG blocking reagent (Vector Laboratories, Burlingame, CA). The primary antibodies were rat monoclonal antiplatelet endothelial cell adhesion molecule-1 (PECAM-1) (MEC 13.3; Santa Cruz Biotechnology, Inc., Santa Cruz, CA) and rabbit polyclonal anti-APJ.<sup>20</sup> The secondary antibodies were biotinylated antirat IgG (Dako Corporation, Carpinteria, CA) and Alexa 568-conjugated anti-rabbit IgG (Molecular Probes, Eugene, OR). Binding of biotinylated antibodies was detected with streptavidin-fluorescein isothiocyanate (FITC) (BD Biosciences, San Diego, CA).

### Quantitative Assessment of CNV Lesion Sizes in Apelin-KO Mice and APJ-KO Mice

Seven days after laser photocoagulation, the eyes were fixed in 4% paraformaldehyde for 30 minutes. Alexa 488-labeled isolectin B4 (Molecular Probes) for apelin-KO mice and FITC-labeled tomato lectin for APJ-KO mice were added to the eye cup and incubated overnight at 4°C. After two washings with Tris-buffered saline, the neuronal retina was detached. The remaining RPE complex was flat mounted in Fluoromount (Diagnostic BioSystems, Pleasanton, CA) and coverslipped. Fluorescent images of the choroidal flat mounts were captured using a fluorescence microscope (AZ-100M; Nikon, Tokyo, Japan). The CNV areas of the WT mice were respectively compared to those of the apelin-KO and APJ-KO mice in choroidal flat mounts.

### Flow Cytometry

Single cells were prepared from the murine CNV lesions. The mice were euthanized 3 days after laser photocoagulation; the eyes were enucleated, and the anterior segment was removed. The posterior segment of each eye, including the sclera,

choroid, and retina, was disrupted with scissors and incubated with collagenase D (20 units/mL) (Roche Diagnostics, Mannheim, Germany) for 45 minutes at 37°C. The digested tissue was filtered through a 40- $\mu$ M cell strainer and suspended in FACS buffer (phosphate buffered saline and 10% fetal bovine serum). Cell suspensions were incubated in Fc block (purified rat anti-mouse CD16/32 monoclonal antibody, 0.5 mg/mL; BD Biosciences) for 15 minutes on ice and stained with phycoerythrin rat antimouse F4/80 antibody (APC; eBioscience, San Diego, CA). Preparations from two eyes were pooled to obtain a sufficient number of viable cells for flow cytometric analysis and were subjected to FACS analysis (FACS Aria II; BD Biosciences). At least 50,000 viable cells were analyzed per condition. Macrophages were defined as F4/80-positive cells.

### Cell Culture

We examined in vitro the correlation between apelin and VEGF and the inflammatory response of apelin, using human umbilical vein endothelial cells (HUVECs) as vascular endothelial cells, which are expressed by APJ and secrete apelin.

The HUVECs were cultured in the EGM Bullet Kit (Takara, Shiga, Japan) containing EGM SingleQuots (Takara) without VEGF. The cells were incubated in their respective conditioning media containing apelin (1  $\mu$ M, [Pyr<sub>1</sub>]-apelin-13; pyroglutamylated C-terminal peptide; Peptide Institute, Osaka, Japan), VEGF (50 ng/mL; R&D Systems, Minneapolis, MN), and lipopolysaccharide (LPS) (200 ng/mL; Wako Pure Chemical Industries, Osaka, Japan), which induced inflammatory responses, respectively, at 37°C. After 24- (apelin and VEGF) and 6-hour (LPS) incubations, the total cellular RNA was processed. Real-time RT-PCR was performed as described previously. The primers and probes for human are listed in the Table.

### Proliferation Assay

The HUVECs were maintained as described previously. Apelin (S78211) and control (4390843) small and interfering RNAs (siRNA) were purchased from Ambion (Austin, TX). The HUVECs were transfected by electroporation using a Nucleofector Kit (Amaya, Cologne, Germany) as previously described.<sup>27</sup> Apelin siRNA-transfected and control siRNA-transfected HUVECs ( $2 \times 10^4$  cells/well) were seeded in 24-well plates and incubated with or without the VEGF receptor inhibitor (SU1498, 10  $\mu$ M/L). In one more experiment, apelin and control siRNA-transfected HUVECs ( $2 \times 10^4$  cells/well) were seeded in 24-well plates. After 24 hours, cells were serum starved (0.3% serum) for 24 hours and then stimulated with VEGF (20 ng/mL) for 24 hours. To assess the proliferation/viability of the endothelial cells, an alamar Blue assay was performed as previously described<sup>28</sup> after 36 hours.

### Statistical Analyses

One-way analysis of variance (ANOVA) followed by Dunnett's test was used to examine the differences in the relative expression levels of each gene. The size of CNV was compared between groups using Student's *t*-test. Difference in macrophage accumulation between WT and KO mice and comparison of proliferation rate in HUVECs between groups were analyzed by two-way ANOVA followed by the Tukey-Kramer test.

## RESULTS

Although physiological retinal vascular development was retarded in apelin-KO mice, capillary length and density were unchanged in retina of apelin-KO compared with that of WT mice at 12 weeks.<sup>16</sup> In addition, there were no differences in

the number of primary or secondary vessel branch points in the limbal vessels of the eye between WT and apelin-KO mice.<sup>16</sup> The choroidal vascularization in apelin-KO and APJ-KO mice in the current study was ophthalmoscopically and histologically normal.

To determine the involvement of the apelin-APJ system in CNV development, real-time RT-PCR was performed to determine the expression patterns of apelin and APJ in the retina-RPE-choroid-sclera complex during CNV development after laser treatment. The apelin expression level peaked on day 2 after laser photocoagulation and gradually returned to baseline after 1 week (1.88  $\pm$  0.23-fold on day 2, 1.05  $\pm$  0.11-fold on day 4, and 0.91  $\pm$  0.09-fold on day 7 versus the control) (Fig. 1A). APJ expression peaked on day 4, and this relatively high expression level was maintained until day 7 (4.71  $\pm$  0.50-fold on day 2, 9.20  $\pm$  1.03-fold on day 4, and 8.92  $\pm$  1.91-fold on day 7) (Fig. 1B). The degree of apelin and APJ mRNA upregulation in the laser-induced CNV murine model was greater than that of VEGF (1.25  $\pm$  0.08-fold on day 2, 1.33  $\pm$  0.06-fold on day 4, and 0.93  $\pm$  0.07-fold on day 7) and VEGF receptor 2 (VEGFR2) (1.68  $\pm$  0.12-fold on day 2, 1.64  $\pm$  0.17-fold on day 4, and 1.43  $\pm$  0.12-fold on day 7) (Figs. 1C, 1D).

To identify the target cells for apelin, we examined APJ localization in the CNV lesions using immunostaining. Immunostaining of RPE/choroid flat mounts and cross sections from the laser-induced CNV model mice 7 days after laser treatment showed that APJ was colocalized with PECAM-1, and the endothelial cells in the choroidal lesions were stained in flat mount (Figs. 2A-C) and cross sections (Figs. 2D-F).

We investigated the role of the apelin-APJ system in CNV development in apelin-KO and APJ-KO mice. Although CNV was observed in apelin-KO mice after laser treatment, the sizes of the CNV lesions seen using Alexa 488-conjugated isolectin B4 7 days after laser treatment significantly decreased by 62.9  $\pm$  14.3% ( $P < 0.05$ ;  $n = 9$  or 10) compared with those in WT mice (Figs. 3A, 3B). We also compared the sizes of the CNV lesions between WT and APJ-KO mice to confirm this result. The size of the CNV lesions significantly decreased in the APJ-KO mice (48.1%  $\pm$  7.1%,  $P < 0.001$ ;  $n = 25-30$ ) compared with the WT mice 7 days after treatment (Figs. 3C, 3D).

To investigate which factors are associated with decreased CNV development after laser application in apelin-KO mice, we examined the inflammatory processes during CNV development in apelin-KO mice. The expression of monocyte chemoattractant protein-1 (MCP-1) and tumor necrosis factor- $\alpha$  (TNF- $\alpha$ ), which induces macrophage infiltration into lesions,<sup>29-33</sup> was significantly upregulated in WT and apelin-KO mice on day 2 after laser treatment (Figs. 4A, 4B). Because macrophage recruitment regulates CNV development,<sup>31-33</sup> we compared the number of infiltrated macrophages between WT and apelin-KO mice using flow cytometry. Since macrophage accumulation peaks on day 3 after laser treatment,<sup>34</sup> we compared the ratio of F4/80-positive cell infiltration on day 3 between the WT and apelin-KO mice. The ratio of F4/80-positive cells at baseline and at day 3 after laser treatment was 0.95  $\pm$  0.08% and 4.77  $\pm$  0.66%, respectively, in WT mice and 0.98  $\pm$  0.10% and 4.65  $\pm$  0.75%, respectively, in apelin-KO mice (Fig. 4C). There was no significant difference in the expression of these factors and macrophage recruitment between the WT and apelin-KO mice. These data suggested that the reduced size of the CNV lesions in apelin-KO mice does not result from less inflammation or macrophage infiltration.

We also found that VEGF and VEGFR2 were upregulated after laser treatment in WT and apelin-KO mice (Figs. 5A, 5B). Similar to results from previous reports using other angiogenic models,<sup>16,20</sup> there was no difference in the upregulation of these genes between WT and apelin-KO mice. These data

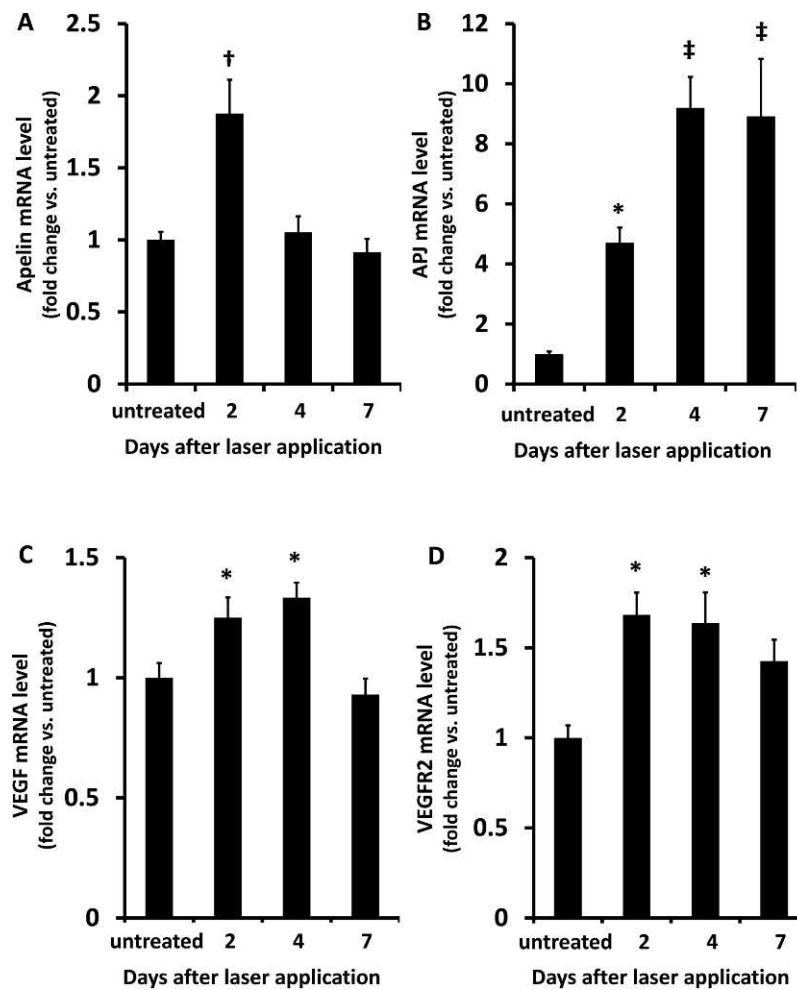


**FIGURE 1.** The gene expression patterns of apelin, APJ, VEGF, and VEGFR2 during CNV development. Quantitative RT-PCR performed in WT mice eyes after laser application ( $n=6$  or  $7$ ). The expression levels of apelin (A), apelin receptor (APJ) (B), VEGF (C), and VEGFR2 (D) are normalized to that of GAPDH. Apelin expression peaks on day 2 after laser application. The APJ expression peaked on day 4, and the high expression was maintained until day 7. \* $P < 0.05$ , † $P < 0.001$ , ‡ $P < 0.0001$  versus untreated. The data are expressed as the mean  $\pm$  standard error of the mean.

suggested that the apelin-APJ system regulates CNV development through the APJ receptor neither by modulating of VEGF and VEGFR2 expression nor by modulating inflammatory factors.

To identify possible crosstalk between the apelin-APJ system and VEGF or inflammatory pathways, we examined the gene expression of the endothelial cells using an in vitro assay. VEGF significantly increased apelin and APJ expression levels in HUVECs at 24 hours (Figs. 6A, 6B) ( $P=0.0060$  and  $P=0.035$ , respectively); however, the VEGF expression level in the HUVECs was unaffected by apelin (Fig. 6C). The apelin and APJ expression levels also were unchanged by LPS treatment, which induces inflammatory cytokine expression, for 6 hours (Figs. 6D, 6E) ( $P=0.87$  and  $P=0.43$ , respectively). Apelin did not affect the expression levels of MCP-1 (Fig. 6F). TNF- $\alpha$  was not detected in HUVECs treated with apelin. These data imply that the apelin-APJ system is likely to be induced by VEGF signaling and not by inflammatory stimulation.

The apelin-APJ system mainly contributes to endothelial cell proliferation during pathological angiogenesis.<sup>20,21,35</sup> Therefore, to assess the individual effects of apelin and VEGF on endothelial cell growth, we evaluated if inhibition of the apelin-APJ system suppresses proliferation of endothelial cells independently of the VEGF/VEGFR2 signaling pathway. We confirmed that apelin siRNA reduced apelin mRNA expression

to 20% and did not affect VEGF mRNA expression in HUVECs. We examined endothelial cell proliferation using the colorimetric alamar Blue assay, which is based on detection of metabolic activity. Apelin siRNA on its own suppressed metabolic activity to  $85.1 \pm 2.3\%$  compared with controls exposed to scrambled siRNA 36 hours after transfection. The VEGFR2 inhibitor SU1498 even suppressed metabolic activity to  $30.4 \pm 1.4\%$  at 36 hours after transfection. Apelin siRNA and SU1498 together suppressed metabolic activity to  $18.5 \pm 1.2\%$  at 36 hours (Fig. 7A). Also, silencing apelin suppressed HUVEC proliferation even under VEGF stimulation (from  $156.9 \pm 1.9\%$  to  $130.0 \pm 0.8\%$ ) (Fig. 7B). Two-way ANOVA revealed no significant interaction between VEGF treatment and apelin silencing, implying that silencing apelin additively inhibits endothelial cell proliferation in the presence or absence of VEGF. These results suggested that apelin-APJ signaling enhances endothelial cell proliferation independently of VEGF signaling.

## DISCUSSION

The current study provided the first evidence that the apelin-APJ system is upregulated during development of CNV lesions in a murine model, that a deficiency of apelin or APJ attenuates

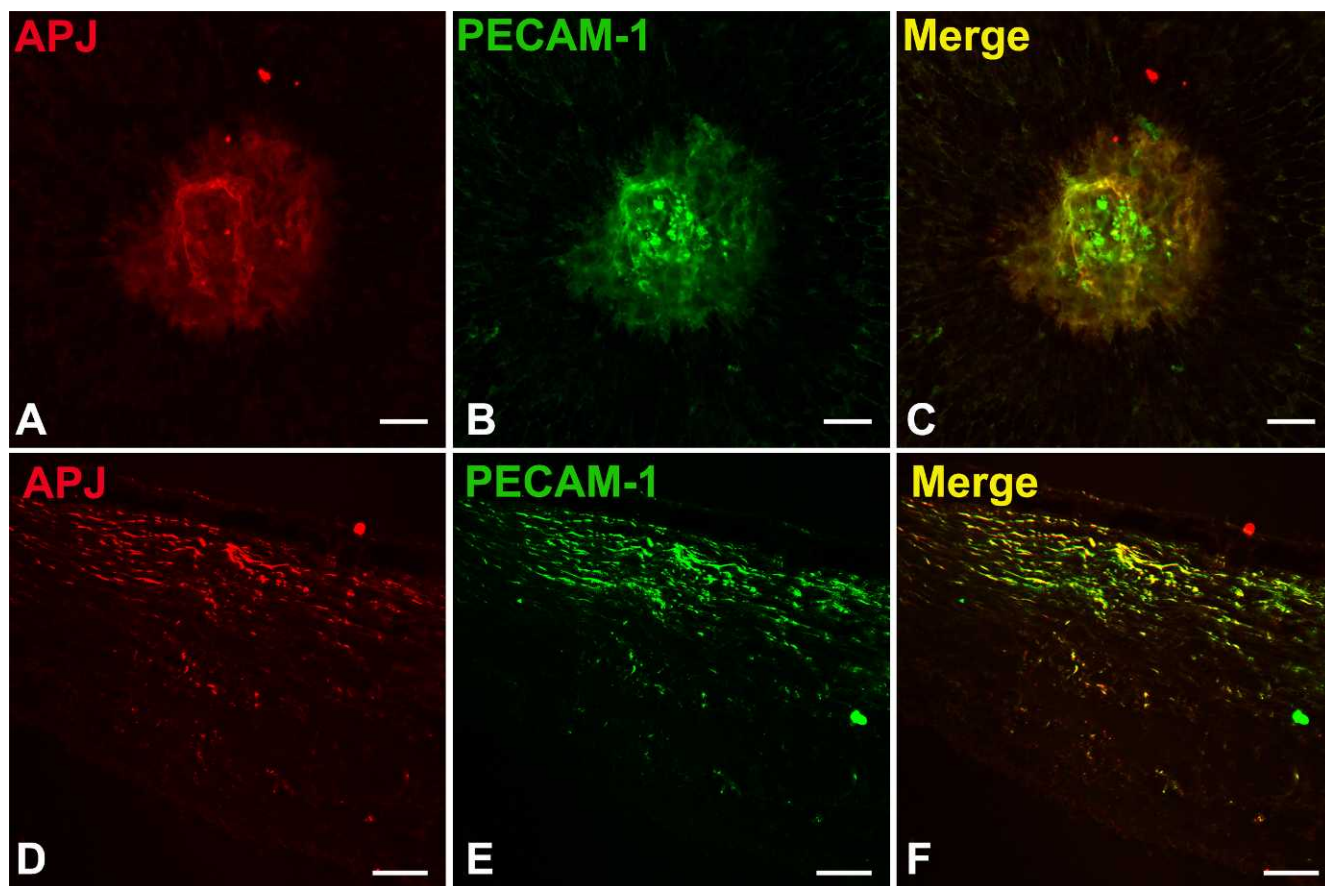


FIGURE 2. APJ expression in the endothelial cells within CNV lesions. APJ (A) and PECAM-1 (B) immunostaining of choroidal flat mounts is shown. APJ is colocalized with PECAM-1 and stained endothelial cells in CNV (C). Double staining of cross section of an eye shows that APJ was colocalized with PECAM-1 in CNV lesions (D-F). Scale bar: 50  $\mu$ m.

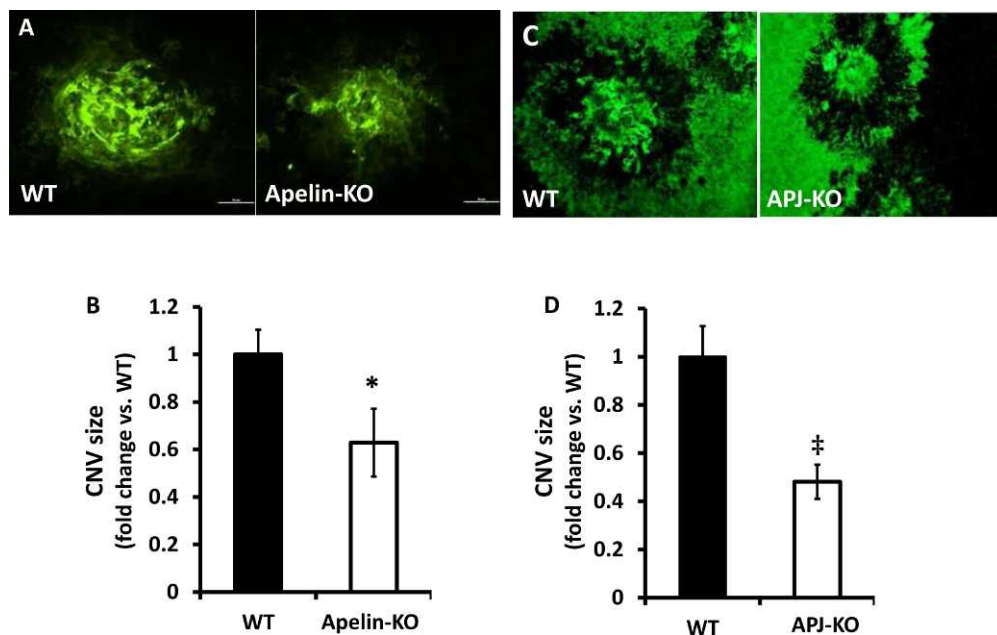
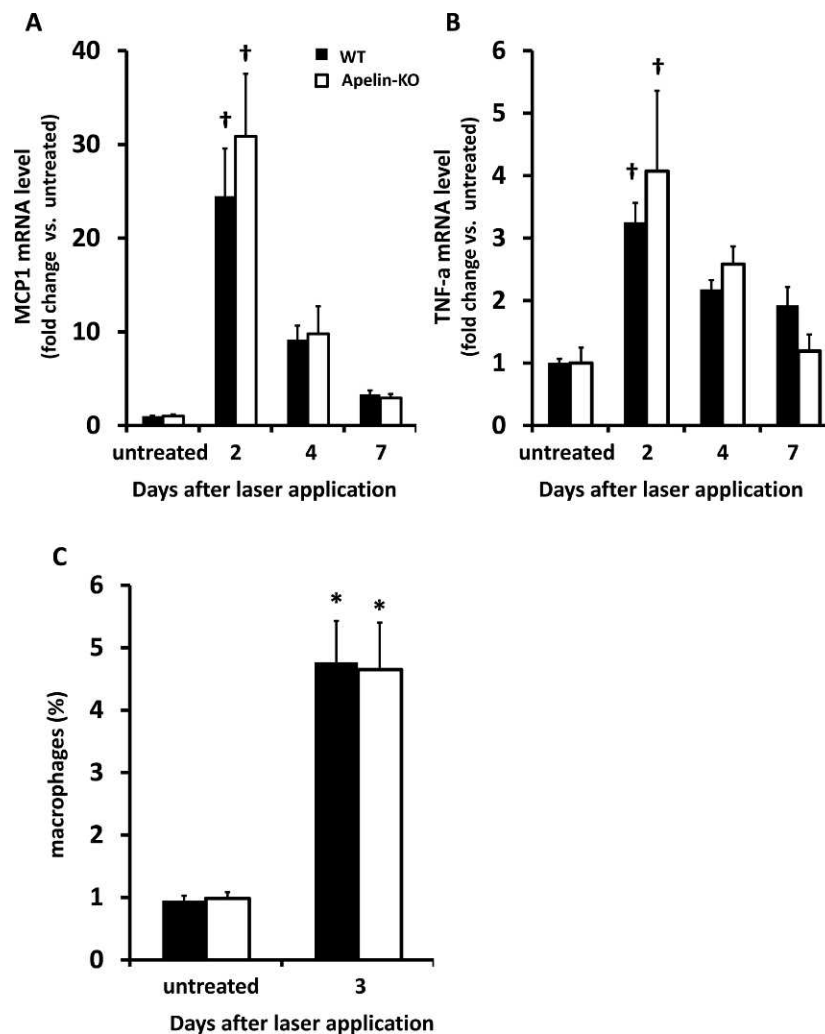


FIGURE 3. A deficiency in the apelin-APJ system attenuates CNV lesions. Representative pictures of the CNV 7 days after laser application in WT and apelin-KO mice (A). Representative pictures from WT and APJ-KO mice (C). The CNV areas in the choroidal flat mounts were measured, and the results of quantitative analysis are shown (B, D). The relative sizes of the CNV in eyes of apelin-KO and APJ-KO mice were 62.9% and 48.1%, respectively, of that in the WT mice. Scale bar: 50  $\mu$ m. \* $P$  < 0.05, ‡ $P$  < 0.001 versus WT. The data are expressed as the mean  $\pm$  standard error of the mean.



**FIGURE 4.** The inflammatory response in apelin-KO mice. Quantitative RT-PCR of the inflammatory factors for WT and apelin-KO mice eyes after laser application ( $n = 6$  or  $7$ ). The expression levels of MCP-1 (A) and TNF- $\alpha$  (B) are normalized to that of GAPDH. The expression levels of both factors peaked on day 2 after laser application in both WT and apelin-KO mice. There was no significant difference between the two mouse models. \* $P < 0.05$ , † $P < 0.001$  versus untreated for each genotype. (C) There was no significant difference in the fraction (%) of macrophages 3 days after laser application between WT and apelin-KO mice. \* $P < 0.05$  versus untreated for each. The data are expressed as the mean  $\pm$  standard error of the mean.

CNV development in mice without reduction of macrophage infiltration, and that apelin enhances endothelial cell proliferation independently of VEGF signaling. Moreover, the expression of apelin and APJ mRNA in the endothelial cells was upregulated by VEGF but not inflammatory factors. These results all strongly suggested that the apelin-APJ system contributes to pathological CNV without affecting macrophage recruitment.

A recent report showed that there was no significant difference in CNV development between WT and apelin-KO mice 2 weeks after laser treatment.<sup>36</sup> However, in our experiments, using a large number of animals and evaluating both apelin-KO mice and APJ-KO mice, we found that laser-induced CNV is decreased in both mouse models at 1 week after laser treatment. The most likely explanation for this discrepancy lies in the difference in time points (1 or 2 weeks) observed. In the laser-induced CNV model, newly formed vessels begin to be enveloped by RPE cells 1 week after laser treatment.<sup>24</sup> By day 10, RPE cells grow over the inner portion of the lesion and by 2 weeks cover the entire CNV.<sup>24,37</sup> If this RPE cell coverage of the lesion is delayed in apelin-KO mice,

then at 2 weeks no significant difference in CNV development between WT and apelin-KO mice may be observed in spite of initially different CNV areas at 1 week after treatment, giving a probable explanation for the contrasting results of the aforementioned and our own study.

Much attention recently has been focused on the possibility that apelin is positively correlated with inflammation in kidney or adipose tissues.<sup>38–41</sup> Both angiogenesis induction and inflammation and immune system activation play critical roles in the pathogenesis of AMD.<sup>42</sup> The VEGF-VEGFR2 pathway is a critical factor<sup>5,6,43–45</sup> in the development of CNV and angiogenesis. Inflammatory processes include macrophage infiltration<sup>31–33,46,47</sup> and the cytokine network.<sup>32,44,45</sup> In the current study, we found no difference between WT and apelin-KO mice in either the expression levels of inflammatory factors or macrophage recruitment during CNV formation. We also showed that VEGF but not TNF in the endothelial cells stimulated expression of the apelin-APJ system. These results imply that the apelin-APJ system may crosstalk with VEGF-VEGFR2 pathways but not inflammatory factors during CNV development.

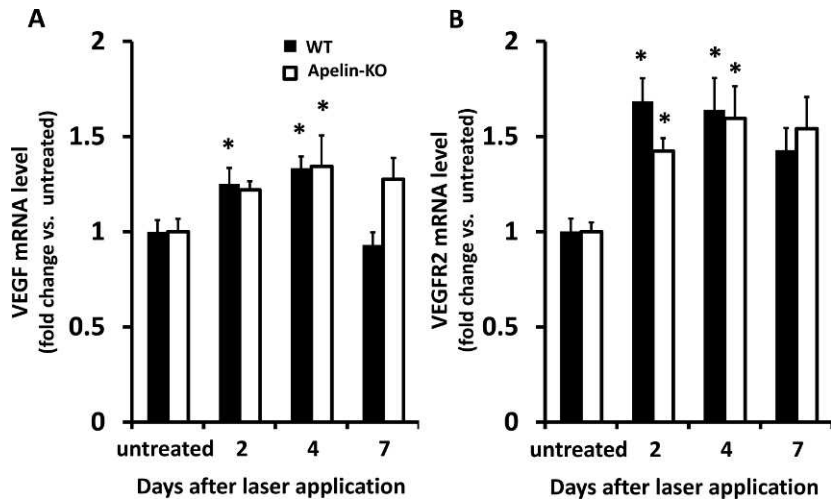


**FIGURE 5.** VEGF signaling expressions in apelin-KO mice. Quantitative RT-PCR of the inflammatory factors for WT and apelin-KO mice eyes after laser application ( $n = 6$  or  $7$ ). The expression levels of VEGF (A) and VEGFR2 (B) are normalized to that of GAPDH. There was no significant difference between the two genotypes. \* $P < 0.05$  versus untreated for each genotype. The data are expressed as the mean  $\pm$  standard error of the mean.

While VEGF signaling modulates apelin and APJ expression, in the current study these signaling pathways stimulated endothelial cell proliferation independently. We showed that apelin siRNA significantly suppressed proliferation of endothelial cells and that inhibition of the apelin-APJ system in combination with SU1498 additively suppressed cellular

proliferation. Additionally, we showed that silencing apelin suppressed cell proliferation even under VEGF stimulation. Consistent with our data, other studies also have reported that although VEGF upregulates apelin and APJ expression in endothelial cells,<sup>14,22,48</sup> apelin and VEGF signaling regulate the size of new vessels independently<sup>22,48</sup> of endothelial cell

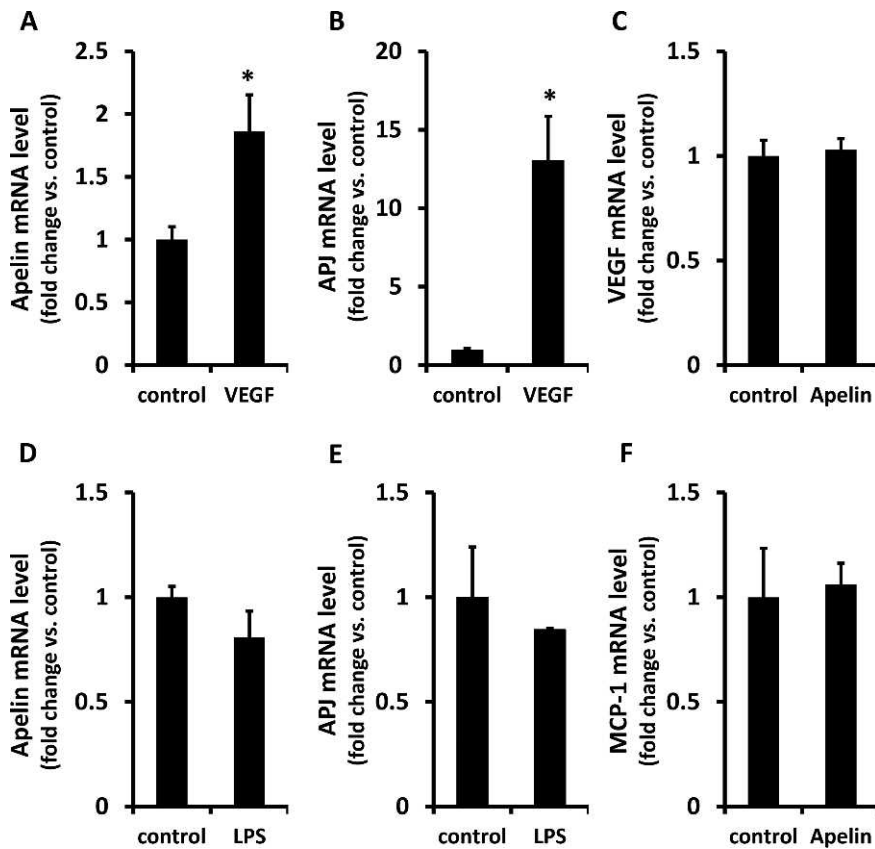


**FIGURE 6.** Crosstalk between the apelin-APJ system and VEGF or inflammatory pathways in vascular endothelial cells. VEGF increased the apelin and APJ expression levels (A, B), but apelin did not increase the VEGF and MCP-1 expression levels (C, F). The apelin and APJ expression levels were unchanged by LPS treatment for 6 hours (D, E). \* $P < 0.05$  versus control. The data are expressed as the mean  $\pm$  standard error of the mean ( $n = 4$ ).

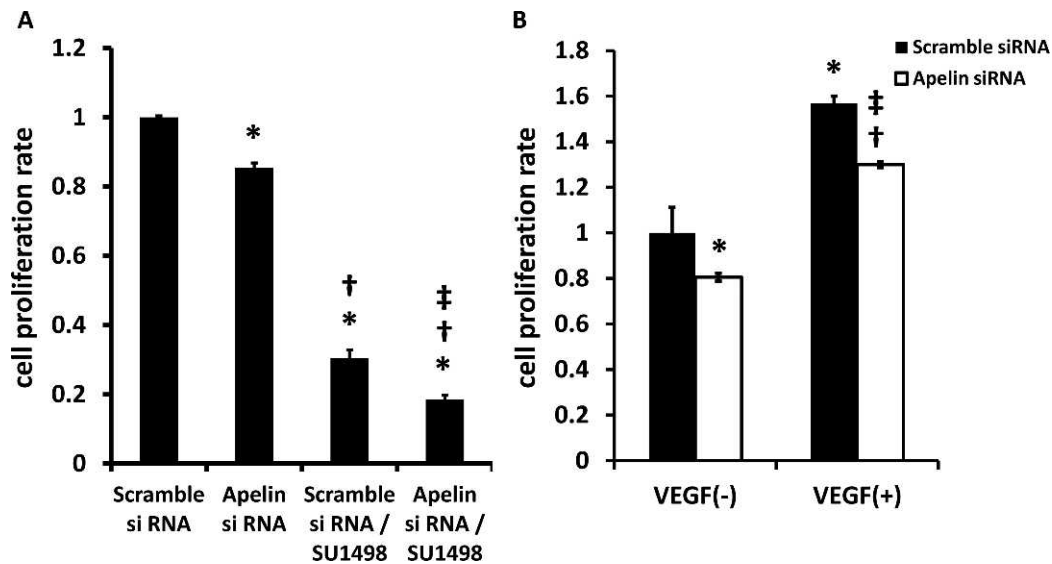


**FIGURE 7.** Apelin siRNA suppressed the endothelial cell proliferation independent of VEGF-VEGFR2 signaling. Proliferation of HUVECs by the alamar Blue assay. **(A)** The apelin siRNA and VEGFR2 inhibitor SU1498 suppress proliferation of endothelial cells ( $n = 6$ ). Both actions suppress endothelial cell proliferation. \* $P < 0.01$  versus scramble siRNA; † $P < 0.01$  versus apelin siRNA; ‡ $P < 0.01$  versus scramble siRNA, SU1498. **(B)** Silencing apelin suppressed HUVEC proliferation even under VEGF stimulation ( $n = 4$ ). \* $P < 0.05$  versus scramble siRNA, VEGF(-). † $P < 0.01$  versus apelin siRNA, VEGF(-). ‡ $P < 0.01$  versus scramble siRNA, VEGF(+). The data are expressed as the mean  $\pm$  standard error of the mean.

proliferation.<sup>20,48</sup> Apelin expression was recently reported to be suppressed by anti-VEGF therapy in a monkey model of central retinal vein occlusion but the extent of the suppression did not parallel that of VEGF.<sup>49</sup> A recent clinical study also reported that the vitreous concentration of apelin in patients with proliferative diabetic retinopathy was significantly higher than in controls but was not associated with the VEGF concentration,<sup>23</sup> and that the expression of apelin mRNA did not correlate with VEGF mRNA in the fibrovascular membrane of patients with retinopathy of prematurity.<sup>50</sup> Taken together, these results indicate a high likelihood that the apelin-APJ system is not a direct downstream signal of the VEGF cascade but is only partially regulated by VEGF.

In summary, the apelin-APJ system may contribute to angiogenesis in the pathology of CNV development, partially independent of the VEGF pathway. Although further experiments are needed to evaluate the therapeutic potential in vivo, the apelin-APJ system might be a promising therapeutic target for inhibiting CNV development in AMD, which insufficiently responds to anti-VEGF therapies.

### Acknowledgments

Supported by Grant-in-Aid for Scientific Research (C) 22591942 (FG) and Grant-in-Aid for Young Scientists (B) 21790098 (AK).

Disclosure: C. Hara, None; A. Kasai, None; F. Gomi, None; T. Satooka, None; S. Sakimoto, None; K. Nakai, None; Y. Yoshioka, None; A. Yamamuro, None; S. Maeda, None; K. Nishida, None

### References

- Green WR. Histopathology of age-related macular degeneration. *Mol Vis.* 1999;5:27.
- Fine SL. Age-related macular degeneration 1969–2004: a 35-year personal perspective. *Am J Ophthalmol.* 2005;139:405–420.
- Argon laser photocoagulation for neovascular maculopathy. Five-year results from randomized clinical trials. Macular Photocoagulation Study Group. *Arch Ophthalmol.* 1991;109:1109–1114.
- Anderson DH, Mullins RF, Hageman GS, Johnson LV. A role for local inflammation in the formation of drusen in the aging eye. *Am J Ophthalmol.* 2002;134:411–431.
- Kvanta A, Algvere PV, Berglin L, Seregard S. Subfoveal fibrovascular membranes in age-related macular degeneration express vascular endothelial growth factor. *Invest Ophthalmol Vis Sci.* 1996;37:1929–1934.
- Ishibashi T, Hata Y, Yoshikawa H, Nakagawa K, Sueishi K, Inomata H. Expression of vascular endothelial growth factor in experimental choroidal neovascularization. *Graefes Arch Clin Exp Ophthalmol.* 1997;235:159–167.
- Kwak N, Okamoto N, Wood JM, Campochiaro PA. VEGF is major stimulator in model of choroidal neovascularization. *Invest Ophthalmol Vis Sci.* 2000;41:3158–3164.
- Heier JS, Brown DM, Chong V, et al. Intravitreal aflibercept (VEGF trap-eye) in wet age-related macular degeneration. *Ophthalmology.* 2012;119:2537–2548.
- Tatemoto K, Hosoya M, Habata Y, et al. Isolation and characterization of a novel endogenous peptide ligand for the human APJ receptor. *Biochem Biophys Res Commun.* 1998;251:471–476.
- Kleinz MJ, Davenport AP. Immunocytochemical localization of the endogenous vasoactive peptide apelin to human vascular and endocardial endothelial cells. *Regul Pept.* 2004;118:119–125.
- del Toro R, Prahst C, Mathivet T, et al. Identification and functional analysis of endothelial tip cell-enriched genes. *Blood.* 2010;116:4025–4033.
- Kim J, Kang Y, Kojima Y, et al. An endothelial apelin-FGF link mediated by miR-424 and miR-503 is disrupted in pulmonary arterial hypertension. *Nat Med.* 2013;19:74–82.
- Kasai A, Shintani N, Oda M, et al. Apelin is a novel angiogenic factor in retinal endothelial cells. *Biochem Biophys Res Commun.* 2004;325:395–400.
- Kalin RE, Kretz MP, Meyer AM, Kispert A, Heppner FL, Brandli AW. Paracrine and autocrine mechanisms of apelin signaling govern embryonic and tumor angiogenesis. *Dev Biol.* 2007;305:599–614.
- Saint-Geniez M, Masri B, Malecaze F, Knibiehler B, Audigier Y. Expression of the murine msr/apj receptor and its ligand

- apelin is upregulated during formation of the retinal vessels. *Mech Dev.* 2002;110:183-186.
16. Kasai A, Shintani N, Kato H, et al. Retardation of retinal vascular development in apelin-deficient mice. *Arterioscler Thromb Vasc Biol.* 2008;28:1717-1722.
  17. Cox CM, D'Agostino SL, Miller MK, Heimark RL, Krieg PA. Apelin, the ligand for the endothelial G-protein-coupled receptor, APJ, is a potent angiogenic factor required for normal vascular development of the frog embryo. *Dev Biol.* 2006;296:177-189.
  18. Sorli SC, Le Gonidec S, Knibiehler B, Audigier Y. Apelin is a potent activator of tumour neovascularization. *Oncogene.* 2007;26:7692-7699.
  19. Berta J, Kenessey I, Dobos J, et al. Apelin expression in human non-small cell lung cancer: role in angiogenesis and prognosis. *J Thorac Oncol.* 2010;5:1120-1129.
  20. Kasai A, Ishimaru Y, Kinjo T, et al. Apelin is a crucial factor for hypoxia-induced retinal angiogenesis. *Arterioscler Thromb Vasc Biol.* 2010;30:2182-2187.
  21. Kunduzova O, Alet N, Delesque-Touchard N, et al. Apelin/APJ signaling system: a potential link between adipose tissue and endothelial angiogenic processes. *FASEB J.* 2008;22:4146-4153.
  22. Kidoya H, Ueno M, Yamada Y, et al. Spatial and temporal role of the apelin/APJ system in the caliber size regulation of blood vessels during angiogenesis. *EMBO J.* 2008;27:522-534.
  23. Tao Y, Lu Q, Jiang YR, et al. Apelin in plasma and vitreous and in fibrovascular retinal membranes of patients with proliferative diabetic retinopathy. *Invest Ophthalmol Vis Sci.* 2010;51:4237-4242.
  24. Tobe T, Ortega S, Luna JD, et al. Targeted disruption of the FGF2 gene does not prevent choroidal neovascularization in a murine model. *Am J Pathol.* 1998;153:1641-1646.
  25. Nakai K, Fainaru O, Bazinet L, et al. Dendritic cells augment choroidal neovascularization. *Invest Ophthalmol Vis Sci.* 2008;49:3666-3670.
  26. Yamada K, Sakurai E, Itaya M, Yamasaki S, Ogura Y. Inhibition of laser-induced choroidal neovascularization by atorvastatin by downregulation of monocyte chemoattractant protein-1 synthesis in mice. *Invest Ophthalmol Vis Sci.* 2007;48:1839-1843.
  27. Secchiero P, Corallini F, Rimondi E, et al. Activation of the p53 pathway down-regulates the osteopontin expression and release by vascular endothelial cells. *Blood.* 2008;111:1287-1294.
  28. Punshon G, Vara DS, Sales KM, Kidane AG, Salacinski HJ, Seifalian AM. Interactions between endothelial cells and a poly(carbonate-silsesquioxane-bridge-urea)urethane. *Biomaterials.* 2005;26:6271-6279.
  29. Shi X, Semkova I, Muther PS, Dell S, Kociok N, Jousen AM. Inhibition of TNF-alpha reduces laser-induced choroidal neovascularization. *Exp Eye Res.* 2006;83:1325-1334.
  30. Noda K, She H, Nakazawa T, et al. Vascular adhesion protein-1 blockade suppresses choroidal neovascularization. *FASEB J.* 2008;22:2928-2935.
  31. Grossniklaus HE, Ling JX, Wallace TM, et al. Macrophage and retinal pigment epithelium expression of angiogenic cytokines in choroidal neovascularization. *Mol Vis.* 2002;8:119-126.
  32. Oh H, Takagi H, Takagi C, et al. The potential angiogenic role of macrophages in the formation of choroidal neovascular membranes. *Invest Ophthalmol Vis Sci.* 1999;40:1891-1898.
  33. Espinosa-Heidmann DG, Suner IJ, Hernandez EP, Monroy D, Csaky KG, Cousins SW. Macrophage depletion diminishes lesion size and severity in experimental choroidal neovascularization. *Invest Ophthalmol Vis Sci.* 2003;44:3586-3592.
  34. Nozaki M, Raisler BJ, Sakurai E, et al. Drusen complement components C3a and C5a promote choroidal neovascularization. *Proc Natl Acad Sci U S A.* 2006;103:2328-2333.
  35. Masri B, Morin N, Cornu M, Knibiehler B, Audigier Y. Apelin (65-77) activates p70 S6 kinase and is mitogenic for umbilical endothelial cells. *FASEB J.* 2004;18:1909-1911.
  36. McKenzie JA, Fruttiger M, Abraham S, et al. Apelin is required for non-neovascular remodeling in the retina. *Am J Pathol.* 2012;180:399-409.
  37. Edelman JL, Castro MR. Quantitative image analysis of laser-induced choroidal neovascularization in rat. *Exp Eye Res.* 2000;71:523-533.
  38. Han S, Wang G, Qi X, Englander EW, Greeley GH Jr. Involvement of a Stat3 binding site in inflammation-induced enteric apelin expression. *Am J Physiol.* 2008;295:G1068-G1078.
  39. Yu S, Zhang Y, Li MZ, et al. Chemerin and apelin are positively correlated with inflammation in obese type 2 diabetic patients. *Chin Med J.* 2012;125:3440-3444.
  40. Malyszko J, Malyszko JS, Pawlak K, Wolczynski S, Mysliwiec M. Apelin, a novel adipocytokine, in relation to endothelial function and inflammation in kidney allograft recipients. *Transplant Proc.* 2008;40:3466-3469.
  41. Daviaud D, Boucher J, Gesta S, et al. TNFalpha up-regulates apelin expression in human and mouse adipose tissue. *FASEB J.* 2006;20:1528-1530.
  42. Penfold PL, Madigan MC, Gillies MC, Provis JM. Immunological and aetiological aspects of macular degeneration. *Prog Retin Eye Res.* 2001;20:385-414.
  43. Lopez PF, Sippy BD, Lambert HM, Thach AB, Hinton DR. Transdifferentiated retinal pigment epithelial cells are immunoreactive for vascular endothelial growth factor in surgically excised age-related macular degeneration-related choroidal neovascular membranes. *Invest Ophthalmol Vis Sci.* 1996;37:855-868.
  44. Amin R, Puklin JE, Frank RN. Growth factor localization in choroidal neovascular membranes of age-related macular degeneration. *Invest Ophthalmol Vis Sci.* 1994;35:3178-3188.
  45. Krzystolik MG, Afshari MA, Adamis AP, et al. Prevention of experimental choroidal neovascularization with intravitreal anti-vascular endothelial growth factor antibody fragment. *Arch Ophthalmol.* 2002;120:338-346.
  46. Sakurai E, Anand A, Ambati BK, van Rooijen N, Ambati J. Macrophage depletion inhibits experimental choroidal neovascularization. *Invest Ophthalmol Vis Sci.* 2003;44:3578-3585.
  47. Tsutsumi C, Sonoda KH, Egashira K, et al. The critical role of ocular-infiltrating macrophages in the development of choroidal neovascularization. *J Leukoc Biol.* 2003;74:25-32.
  48. Kidoya H, Naito H, Takakura N. Apelin induces enlarged and nonleaky blood vessels for functional recovery from ischemia. *Blood.* 2010;115:3166-3174.
  49. Zhao T, Lu Q, Tao Y, Liang XY, Wang K, Jiang YR. Effects of apelin and vascular endothelial growth factor on central retinal vein occlusion in monkey eyes intravitreally injected with bevacizumab: a preliminary study. *Mol Vis.* 2011;17:1044-1055.
  50. Zhang Y, Jiang YR, Lu Q, Yin H, Tao Y. Apelin in epiretinal fibrovascular membranes of patients with retinopathy of prematurity and the changes after intravitreal bevacizumab. *Retina.* 2013;33:613-620.